Response to Referee 2 on egusphere-2024-3251

First, we would like to thank the Referee for reviewing and commenting on the manuscript, which will improve the quality of the manuscript. Please find the item-by-item reply below, with the responses in blue. All the suggested changes will be implemented in the revised text that will be uploaded.

Referee comments

The study provides valuable insights into firn properties using altimetry data from CryoSat-2 (CS2) and ICESat-2 (IS2), but there are several areas that need clarification and refinement to validate the conclusions. Before any major insight or conclusion can be drawn I find that there are several aspect of the methodology that needs more validation or attention to ensure the accuracy of the results. Except that I find that its a very interesting approach that can yield some good scientific insight into this area.

Below are detailed comments and suggestions to help improve the study with a focus on the main methodology for the altimetry components and firn models.

General Comments

LeW Computation:

In Figure 1 (related to L87), it is clear that using thresholds at 0.01 and 0.99 may result in unrealistic LeW values unrelated to the volume/surface scattering ratio. How exactly is LeW computed? Is a peak finder algorithm employed? I strongly suggest either smoothing the waveform for better LeW extraction or using the Offset Center of Gravity (OCOG) method to compute the width after identifying the leading edge. Alternatively, the overall OCOG amplitude could serve as the max. The critical objective is to minimize jitter in the LeW estimation. A specific example is pixel C, where the algorithm identifies a maximum beyond the true leading edge, likely near bin 40–45, which aligns with observations for pixel A.

We directly normalised each waveform using the maximum power and searched for the first bin (except for the initial noisy bins) that exceeds 0.01 and the last bin that exceeds 0.99 of the normalised waveform. We agree with the recommendations of the referee, and will improve the method in the revised manuscript. From here onwards, we compute the OCOG amplitude to serve as the maximum power, and following another one of the referee's comments below, we define the beginning and the end of the leading edge using thresholds at 0.05 and 0.95.

In addition, in response to one of the comments below, we adopted Baseline E data, and the results shown in this document will be based on Baseline E instead of Baseline D. Accordingly, the time series of our study have been extended from 2011—2021 to 2010—2024.

DEM (Section 2.3)

The REMA description should be moved to the beginning of the data description section. Introducing it first provides essential context, as the DEM is referenced throughout both the CS2 and IS2 sections.

This will be implemented in the revised manuscript.

FDM (Section 2.4)

Given the availability of multiple firn models such as GSFC and GEMB, have you compared their results against the IMAU-FDM model? Previous analyses have shown substantial spatial and temporal differences among these models, which I think is crucial when evaluating penetration depth from laser and radar measurements. At a minimum, a discussion on the potential impact of model differences is necessary to gauge the validity of the results.

Furthermore, models like GSFC and GEMB have been updated to include data through the end of 2024, which presents a valuable opportunity to extend your CS2 and IS2 time series analysis. Incorporating these more recent datasets will enhance the robustness of your study and help provide more insight into how melt events affect the LeW and elevation relationships.

While we agree with the reviewer that comparing the altimetry results with more firn models would strengthen our analysis, we do not do this for the following reasons:

1) We believe that adding more firn models to our analysis has little added benefit. We already make use of two different models, driven by two different RCMs (IMAU-FDM and MAR's firn module). While the models differ in their exact density, temperature and water content, they qualitatively agree in their response to 2012's melt season, the subsequent drier years, and increased melt after 2018. The focus in this paper is on the latter and different firn models would show similar trends. This makes sense, as these trends are largely driven by the climate and not the firn physics. We explicitly refrain from making quantitative statements that would not be supported by a single firn model.
2) A comparison of the performance of different firn models is out of the scope of this work. IMAU-FDM's capabilities have already been compared to other models under idealised non-melt conditions (Lundin et al., 2017), melting conditions (Vandecrux et al., 2020) and runoff capabilities (Machguth et al., under review).
3) Finally, there is a simple practical reason for not including GEMB and GSFC in our analysis: the mean density of the uppermost 1,5 m of firn, which is used extensively in our analysis, is not publicly available online for either model, whereas IMAU-FDM's and MAR's data was already available to the authors. While we could have asked the developers of GEMB and GSFC to also provide us with these data sets, we decided against this given the reasons above and include the potential of GEMB and GSFC in Discussion.

Resolution (Sections 3.1, 3.2, and 3.3):

The current 50x50 km binning resolution seems excessively coarse and likely introduces decorrelation, especially for the "dz" variable but also to elevation as you are mixing a lot of different elevations regions. Increasing the spatial resolution would likely improve both spatial and temporal patterns and correlations.

The in creased spatial resolution of 10kmx10km will be implemented in the revised manuscript.

Correlation (Section 4.3):

The low correlation values (~0.3) are surprising, especially when using a 50% threshold, which should generally yield higher correlations due to its more sensitive to volume change. I remember seeing much larger correlations in both Antarctica and Greenland using the same methodology you have provided. A few factors may contribute to this, including the coarse resolution and the LEPTA slope correction method. LEPTA may inadvertently remove signal by basing its correction on leading-edge range information that varies over time. Testing a more traditional slope correction method, as suggested you explained in Li et al. (2022), would help to better understand this. Additionally, localized analyses are likely to reveal higher correlations, as elevation usually de-correlates a lot more over larger distance while LeW might have larger spatial cohesion.

We appreciate the referee for pointing out the problem. First of all, we realised that the problem lies indeed in our original intuitive LeW estimation, where we directly used 0.01 and 0.99 thresholds to cut the normalised waveform. After following the referee's suggestions to use the OCOG amplitude as the maximum amplitude and using 0.05 and 0.95 thresholds, the correlation between LeW and dh improved to approximately 0.6 (Fig. R1 in blue). Each pixel has the resolution of 25km x 25km.

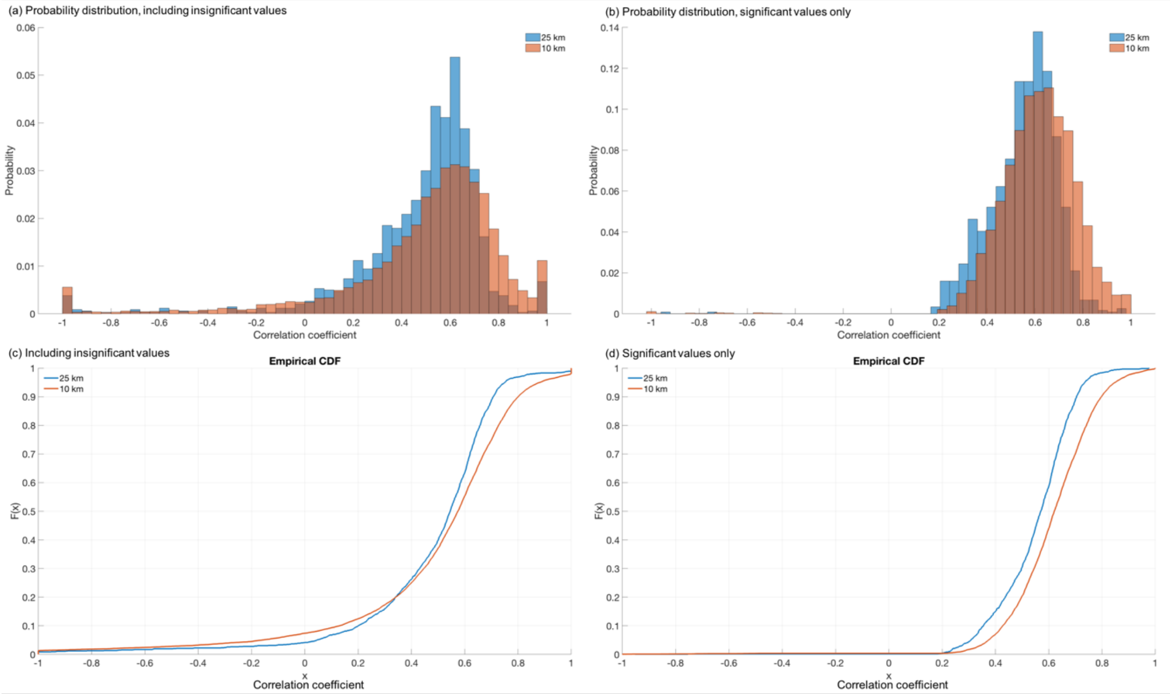

Figure R1. (a)—(b) Probability distribution histogram and, (c)—(d) cumulative distribution function of correlation coefficients when using the improved LeW estimation and different grid resolutions. (a) and (c) include all correlation coefficients. (b) and (d) only use the correlation coefficients with p-values not higher than 0.05.

To inspect the effect of different resolutions, we used a 10km x 10km grid to derive the correlation coefficients and inspected the results. In order to provide a more straightforward assessment, we compare the histogram of correlation coefficient using different resolutions, as shown in Fig. R1. It is true that according to the probability distribution, the number of pixels with correlation coefficients higher than 0.75 increased, compared to the 25km x 25km case. In addition, both resolutions result in insignificant (p-value > 0.05) correlation coefficients towards the Greenland coastal regions. Therefore, we remove the insignificant values and evaluate the probability and cumulative distribution function (CDF), as shown in Fig. R1b and d. After removing the insignificant values, it is more apparent that the correlation coefficients derived using the 10km x 10km resolution is more concentrated above 0.7, while those derived using the 25km x 25km resolution is only concentrated between 0.5 and 0.7.

Finally, we also inspect whether using the traditional slope method (Bamber, 1994) and the point-based method (Roemer et al., 2007) can further improve the correlation. For this comparison, we show the map of correlation coefficients in Fig. R2, using the 10km x 10km grid determined above. The figure shows that the slope method only results in high correlation between LeW and dh in the Greenland interior with little topography, and the point-based method results in slightly lower (~0.5) correlation coefficients than LEPTA. Our explanation is as follows. The height estimations from LEPTA method best represents the laser-radar height offsets, which in turn indicates the volume scattering effects. This can be also reflected by LeW, which varies due to the variation in volume scattering. The slope method, on the contrary, does include the topography signal that theoretically also has an impact on LeW. However, its implication of the laser-radar height offsets can be compromised, as it introduces the uncertainties caused by the simple assumption that the topography within the radar pulse-limit footprint can be represented by a slope. Similarly, the point-based method may also suffer from the simplication of a fixed footprint size, resulting a slightly less ideal derived dh, as shown in Li et al. (2022).

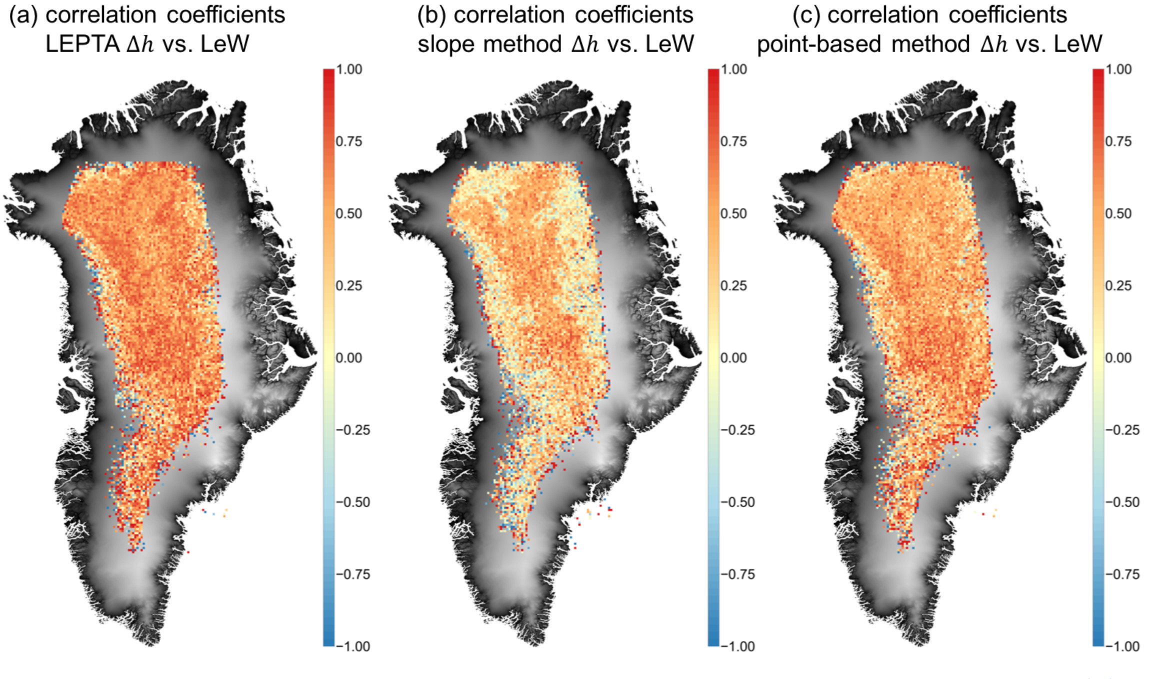

Figure R2. Comparison of correlation coefficients between LeW and dh derived using (a) LEPTA, (b) slope method (Bamber, 1994; Li et al., 2022), and point-based method (Roemer et al., 2007; Li et al., 2022).

Therefore, we believe that 0.6 is a sufficiently high correlation coefficient between dh and LeW, as it on the one hand indicates that LeW increases simultaneously with the laser-radar height offset, indicating an increased volume scattering. On the other hand, it is also consistent with the observation of Nilsson et al. (2015), where the extreme melt event has a more prolonged effect on LeW than other parameters derived by a satellite radar altimeter.

Specific Comments

L54: The Nilsson et al. (2015) study was not limited to NEEM; it covered the entire LRM region, although the time series presented was from NEEM.

This will be changed from

"Despite the advances in using altimetry to monitor Greenland's firn, the evaluation of firn properties has been limited to either to periods without extensive melt (e.g. January 2013 to January 2019; Scanlan et al., 2023) or small regions (e.g., NEEM site; Nilsson et al., 2015)."

to

"Despite the advances in using altimetry to monitor Greenland's firn, the evaluation of firn properties has been limited to either to periods without extensive melt (e.g. January 2013 to January 2019; Scanlan et al., 2023) or a short period right after the 2012 melt (e.g., up to 2014; Nilsson et al., 2015). The firn condition in a longer term, especially following the 2019 melt (Tedesco and Fettweis, 2020) melt, needs to be better monitored."

in the revised manuscript.

L59: Provide a theoretical penetration depth for Ku-band frequencies. For Ku-band over the Greenland Ice Sheet (GrIS), penetration depth is typically 1-2 meters. Additionally, mention that the bias is retracker-dependent.

We will add

"The penetration bias is typically 1-4 metres over the Greenland Ice Sheet (Slater et al., 2019), depending on the firn status (e.g. dry, wet, refrozen) and the retracker (Michel et al., 2014; Simonsen and Sørensen, 2017; Li et al., 2022)"

in the revised manuscript.

L85: Consider updating to Baseline-E, as it includes significant improvements in waveform processing compared to Baseline-D.

Thoughout this document, the results are generated using Baseline E data (as mentioned in the comments above). These updated results will be presented in the revised manuscript.

L87: The 0.01 threshold for LeW seems too low; most studies use thresholds between 0.05 and 0.15 to account for noise. What is the impact of changing these values to 0.05 and 0.95? A more robust approach would be to compute LeW using OCOG parameters, which are less sensitive to noise.

When we aim to observe the temporal variation of LeW, changing the 0.01 threshold to 0.05 did not result in essential changes. However, following the general comment and this specific comment of the referee, we will implement the more conventional and robust approaches in the revised manuscript.

L91: The 50% threshold is appropriate for focusing on volume scattering rather than surface scattering. However, the LeW extraction algorithm needs to be redefined or better explained. OCOG-based methods would offer greater robustness.

This will be updated in the revised manuscript (as mentioned in the comments above).

L98: Include a map figure or inset to indicate pixel locations, as their current placement is unclear to the reader.

The pixel locations should be the same one as in Fig. 3, which did not appear in L98 yet. We agree that the current description is unclear and this will be better arranged in the revised manuscript.

L103: Justify the use of a 50x50 km binning resolution, as it appears excessively coarse. Correlation length analysis could support this choice, or consider aligning the resolution with firn models, which typically have a 10 km resolution. If empty pixels result from a 10 km grid, they can be filled using gentle interpolation.

This choice was originally used in Li et al. (2022) to ensure that every inspected pixel should have sufficient (more than 10) data points to compute the reliable statistics, i.e. mean, median and standard deviation. We admit that this was an intuitive choice, therefore we have implemented different pixel sizes (50km x 50km, 25km x 25km, and 10km x 10km) to generate LeW time series, and show the results in Fig. R3. For each sub-plot, y-axis shows the distance along the north-south transect. The overall spatio-temporal patterns of using different resolutions are similar, while the 25km x 25km and 10km x 10km time series indeed show better details.

Finally, due to the higher correlation coefficients between dh and LeW using the 10km x 10km resolution (as assessed above) and the consistency with firn models, we will adopt the 10km x 10km resolution in the revised manuscript.

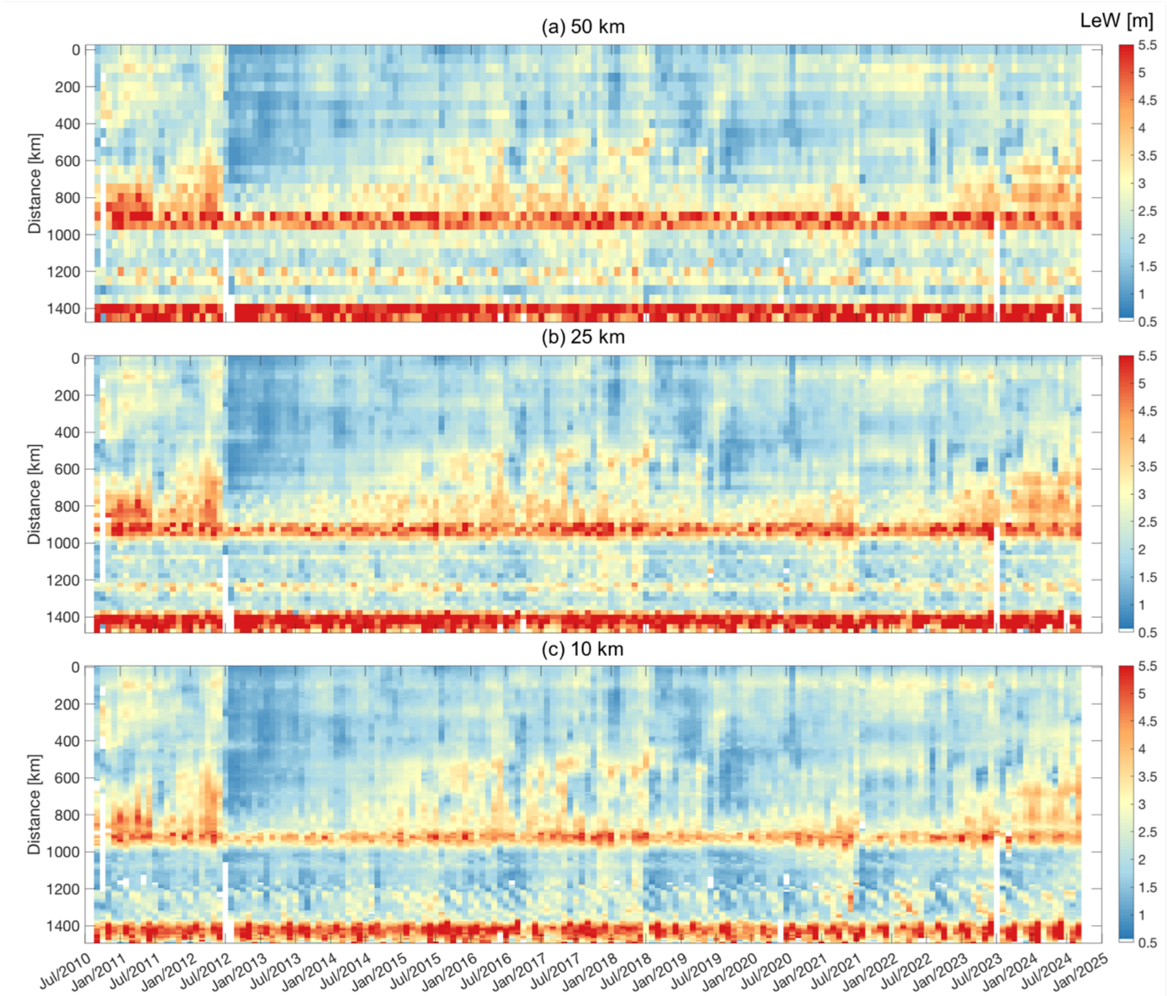

Figure R3. Comparison of LeW time series along the north-south transect when different resolutions are adopted.

L117: The DEM resolution (100 m) and search radius (50 m) may not be optimal. Wouldn't this setup yield identical DEM values for adjacent locations? A higher-resolution DEM (e.g., 10 m from REMA) would likely provide more accurate results, particularly in areas with complex topography.

We appreciate the suggestion. However, from Li et al. (2022), we found that loading the ArcticDEM with a resolution higher than 100 m was not feasible in MATLAB. One solution would be to crop the DEM, but this was not convenient for the processing chain, therefore we adopted 100 m as the finest resolution in our sensitivity analysis.

Reference

Bamber, J. L.: Ice sheet altimeter processing scheme, International Journal of Remote Sensing, 15, 925–938, https://doi.org/10.1080/01431169408954125, 1994.

Li, W., Slobbe, C., and Lhermitte, S.: A leading-edge-based method for correction of slope-induced errors in ice-sheet heights derived from radar altimetry, The Cryosphere, 16, 2225–2243, https://doi.org/10.5194/tc-16-2225-2022, 2022.

Lundin, J. M. D, Stevens, C. M., Arthern, R., Buizert, C., Orsi, A., Ligtenberg, S. R. M., Simonsen, S. B., Cummings, E., Essery, R., Leahy, W., Harris, P., Helsen, M. M., and Waddington, E., D.: Firn Model Intercomparison Experiment (FirnMICE), Journal of Glaciology, 63(239), 401-422, https://doi.org/10.1017/jog.2016.114, 2017.

Machguth, H., Tedstone, A., Kuipers Munneke, P., Brils, M., Noël, B., Clerx, N., Jullien, N., Fettweis, X., and van den Broeke, M.: Runoff from Greenland's firn area – why do MODIS, RCMs and a firn model disagree?, EGUsphere [preprint], https://doi.org/10.5194/egusphere-2024-2750, 2024.

Nilsson, J., Vallelonga, P., Simonsen, S. B., Sørensen, L. S., Forsberg, R., Dahl-Jensen, D., Hirabayashi, M., Goto-Azuma, K., Hvidberg, C. S., Kjaer, H. A., and Satow, K.: Greenland 2012 melt event effects on CryoSat-2 radar altimetry, Geophysical Research Letters, 42, 3919–3926, https://doi.org/10.1002/2015gl063296, 2015.

Roemer, S., Legrésy, B., Horwath, M., and Dietrich, R.: Refined analysis of radar altimetry data applied to the region of the subglacial Lake Vostok/Antarctica, Remote Sens. Environ., 106, 269–284, https://doi.org/10.1016/j.rse.2006.02.026, 2007.

Simonsen, S. B. and Sørensen, L. S.: Implications of changing scattering properties on Greenland ice sheet volume change from Cryosat-2 altimetry, Remote Sensing of Environment, 190, 207–216, https://doi.org/10.1016/j.rse.2016.12.012, 2017.

Slater, T., Shepherd, A., Mcmillan, M., Armitage, T. W. K., Otosaka, I., and Arthern, R., J.: Compensating Changes in the Penetration Depth of Pulse-Limited Radar Altimetry Over the Greenland Ice Sheet, IEEE Transactions on Geoscience and Remote Sensing, vol. 57, no. 12, 9633-9642, https://doi.org/10.1109/TGRS.2019.2928232, 2019.

Tedesco, M. and Fettweis, X.: Unprecedented atmospheric conditions (1948–2019) drive the 2019 exceptional melting season over the Greenland ice sheet, The Cryosphere, 14, 1209–1223, https://doi.org/10.5194/tc-14-1209-2020, 2020.

Vandecrux, B., Mottram, R., Langen, P. L., Fausto, R. S., Olesen, M., Stevens, C. M., Verjans, V., Leeson, A., Ligtenberg, S., Kuipers Munneke, P., Marchenko, S., van Pelt, W., Meyer, C. R., Simonsen, S. B., Heilig, A., Samimi, S., Marshall, S., Machguth, H., MacFerrin, M., Niwano, M., Miller, O., Voss, C. I., and Box, J. E.: The firn meltwater Retention Model Intercomparison Project (RetMIP): evaluation of nine firn models at four weather station sites on the Greenland ice sheet, The Cryosphere, 14, 3785–3810, https://doi.org/10.5194/tc-14-3785-2020, 2020.